Fault-Tolerant Linear Optical Quantum Computing with Small-Amplitude Coherent States

A. P. Lund,[1,*] T. C. Ralph,[1] and H. L. Haselgrove[2,3]

[1]*Centre for Quantum Computer Technology, Department of Physics, University of Queensland, St. Lucia, QLD 4072, Australia*
[2]*C3I Division, Defence Science and Technology Organisation, Canberra, ACT 2600, Australia*
[3]*School of Information Technology and Electrical Engineering, University of New South Wales at ADFA, Canberra 2600 Australia*

(Received 20 June 2007; published 25 January 2008)

Quantum computing using two coherent states as a qubit basis is a proposed alternative architecture with lower overheads but has been questioned as a practical way of performing quantum computing due to the fragility of diagonal states with large coherent amplitudes. We show that using error correction only small amplitudes ($\alpha > 1.2$) are required for fault-tolerant quantum computing. We study fault tolerance under the effects of small amplitudes and loss using a Monte Carlo simulation. The first encoding level resources are orders of magnitude lower than the best single photon scheme.

DOI: 10.1103/PhysRevLett.100.030503 PACS numbers: 03.67.Lx, 42.50.−p

Linear optical quantum computing uses off-line resource states, linear optical processing, and photon resolving detection to implement universal quantum processing on optical quantum bits (qubits) [1]. This technique avoids a number of serious problems associated with the use of in-line nonlinearities for quantum information processing including their limited strength, loss, and inevitable distortions of mode shape by the nonlinear interaction. The trade-off for adopting the linear approach has been large overheads in resource states and operations. In the standard approach, which we will refer to as linear optical quantum computing (LOQC) [2], single photons are used as the physical qubits. Although progress has been made in reducing the overheads [3], for a fault-tolerant operation they remain very high [4].

An alternative version of linear optical quantum computing, coherent state quantum computing (CSQC) [5], uses coherent states for the qubit basis. This is an unusual approach as the computational basis states are not energy eigenstates and are only approximately orthogonal. Previous work on CSQC has concentrated on the regime where coherent states are relatively large ($\alpha > 2$) and the orthogonality is practically zero. It has been shown that CSQC has resource-efficient gates [6].

In this Letter we show how to build nondeterministic CSQC gates for arbitrary amplitude coherent states that are overhead efficient and (for $\alpha > 1.2$) can be used for fault-tolerant quantum computation. We estimate the fault-tolerant threshold for a situation in which photon loss and gate nondeterminism are the dominant sources of error. As our gates operate for any amplitude coherent states, proof of principal experiments are possible using even smaller amplitudes. Given recent experimental progress in generating the required diagonal resource states [7] we suggest that CSQC should be considered a serious contender for optical quantum processing.

For this Letter we use the CSQC qubit basis $|0\rangle = |\alpha\rangle$, $|1\rangle = -|\alpha\rangle$, where $|\alpha\rangle$ describes a coherent state with (real) amplitude α (i.e., $\hat{a}|\alpha\rangle = \alpha|\alpha\rangle$). These states do not define a standard qubit basis for all α as $\langle -\alpha|\alpha\rangle = e^{-2\alpha^2} \neq 0$, but for $\alpha > 2$ this overlap is practically zero [5]. A general CSQC single-qubit state is

$$N_{\mu,\nu}(\alpha)(\mu|\alpha\rangle + \nu|-\alpha\rangle), \tag{1}$$

where $N_{\mu,\nu}(\alpha)$ normalizes the state and depends on the coefficients of the state. A special case is the diagonal states with $\mu = \pm\nu$ which can be written as $|\pm\rangle = N_{1,\pm 1}(\alpha)(|\alpha\rangle \pm |-\alpha\rangle)$. These states form the resource used when constructing CSQC gates using linear optics and photon detection. The diagonal state with a plus (respectively, minus) sign has even (odd) symmetry and contains only even (odd) Fock states. This means that a diagonal (i.e., X-basis) measurement can be performed by a photon counter and observing the parity.

The computational or Z-basis measurement is shown in Fig. 1(a) and the Bell state measurement is shown in Fig. 1(b). The Z basis and Bell state measurements must distinguish between nonorthogonal states. For the measurement to be unambiguous and error-free, it must have a failure outcome [10]. This occurs in both measurements when no photons are detected. The probability of failure tends to zero as α increases.

A critical part of constructing CSQC gates for all α is teleportation [5,9]. This is shown in Fig. 1(c). As the teleporter uses unambiguous Bell state measurements there are 5 outcomes to the measurement. Four outcomes correspond to successfully identifying the respective Bell states. When the appropriate Pauli corrections are made the input qubit is successfully transferred to the output. The fifth outcome corresponds to the measurement failure whose probability again decreases to zero as α increases. Upon failure the output of the teleporter is unrelated to the input and hence the qubit is erased. It is this ability to unambiguously teleport the qubit value, in spite of the fact that the basis states are nonorthogonal, that is key to the success of our scheme.

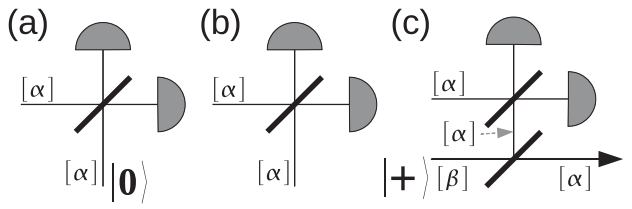

FIG. 1. Schematics for unambiguous CSQC (a) Z basis, (b) Bell state measurements, and (c) CSQC teleportation. Thin lines represent modes whose state is a CSQC qubit with the encoding amplitude shown near each line in square brackets. Prepared CSQC qubit states are shown in the logical basis with the boldface font. The Z-basis measurement in (a) as described in [8] is performed by determining which mode photons are present. The Bell state measurement in (b) as described in [5] is performed by determining which mode photons are in and how many photons are present. Both these measurements fail when no photons are present. (c) shows how CSQC teleportation [5,9] is achieved. A Bell state is generated by splitting a $\beta = \sqrt{2}\alpha$ diagonal state on a beam splitter and performing a Bell state measurement on an unknown qubit and one-half of this entangled state. All detectors are photon counters, all beam splitters are 50:50, and all unlabeled inputs are arbitrary CSQC qubit states.

Unitary transformations on a CSQC qubit as defined in Eq. (1) will not reach all transformations required to do quantum computing. This is because unitary transformations preserve inner products while various transformations that we might wish to implement (e.g., $|\pm\alpha\rangle \rightarrow |\alpha\rangle \pm |-\alpha\rangle$) do not. We implement our gates using nonunitary, measurement-induced gates which act like unitary gates on the coefficients of our CSQC qubits for all α. This requires gates which have in general a nonzero probability of failure.

We construct a universal set of gates that allows us to implement error correction in a standard way. Our objective is to use the error correction to deal with gate failure errors. Unlike the gates introduced in [5] our gates work for all values of α.

We choose our universal set of quantum gates as a Pauli X gate, an arbitrary Z rotation [i.e., $Z(\theta) = e^{i(\theta/2)Z}$], a Hadamard gate, and a controlled-Z gate.

In CSQC the X gate is the only gate deterministic for all α. The gate is performed by introducing a π phase shift on the qubit [5]. The remainder of the gates are implemented via quantum gate teleportation [11]. Just as we are able to implement unambiguous state teleportation, we are able to implement unambiguous gate teleportation. The gates are implemented by altering the form of the entanglement used in the teleporter. The Z rotation is achieved by using the entangled state $e^{i\theta/2}|\alpha, \alpha\rangle + e^{-i\theta/2}|-\alpha, -\alpha\rangle$, the Hadamard gate uses the entangled state $|\alpha, \alpha\rangle + |\alpha, -\alpha\rangle + |-\alpha, \alpha\rangle - |-\alpha, -\alpha\rangle$, and the controlled-$Z$ gate uses the four qubit entangled state $|\alpha, \alpha, \alpha, \alpha\rangle + |\alpha, \alpha, -\alpha, -\alpha\rangle + |-\alpha, -\alpha, \alpha, \alpha\rangle - |-\alpha, -\alpha, -\alpha, -\alpha\rangle$ which is used as the shared entanglement of two teleporters. The controlled-Z entanglement can be generated from the Hadamard entanglement with coherent state amplitude $\sqrt{2}\alpha$ by splitting the outputs at 50:50 beam splitters. Hadamard and Z-rotation entanglement generation are shown in Fig. 2.

Depending on the outcome of the Bell state measurement in a teleported gate, it may be necessary to apply an X and/or Z Pauli operator to the output. In this Letter, we assume that these Pauli operators are not applied directly, but rather absorbed into the error-correction process via the Pauli frame technique [12]. If the outcome of the Bell state measurement is failure, then we say the gate failed and the qubit on which it acted upon is erased.

In calculating a noise threshold [13] for CSQC it is necessary to establish a model for the noise experienced by each operation (i.e., gates, measurements, and preparations). This model is expressed in terms of two parameters: the qubit amplitude α and a loss parameter η (see below). We use this model to simulate concatenated fault-tolerant error-correction protocols. A particular setting of the parameters (α, η) is said to be below the threshold if the rate of uncorrectable errors is observed to decrease to zero as more levels of error correction are applied. Here we calculate the threshold curve, defined to be the curve through the α-η plane which lies at the boundary between the sets of parameters that are above and below the threshold.

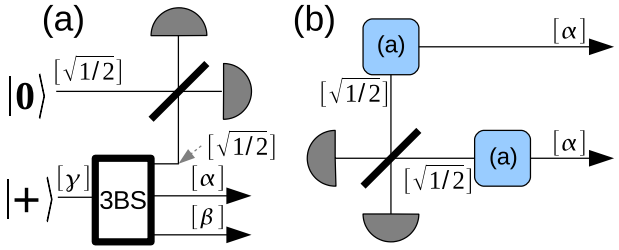

FIG. 2 (color online). Schematics for gate entanglement generation with the same layout as in Fig. 1. (a) shows Z-rotation entanglement preparation. A $|+\rangle$ state with amplitude $\gamma = \sqrt{\alpha^2 + \beta^2 + 1/2}$ is split at a three way beam splitter (3BS) generating the state $|\alpha', \alpha, \beta\rangle + |-\alpha', -\alpha, -\beta\rangle$, where $\alpha' = 1/\sqrt{2}$ and $\beta = \alpha$ for the rotation. The α' mode is mixed at a beam splitter with reflectivity $\cos^2(\frac{\theta}{2})$ with a coherent state of equal amplitude. The two output modes are then detected and the output is accepted if one photon is measured in total (probability of success approximately 0.3). (b) shows the Hadamard entanglement preparation. Two copies of the entanglement from (a) are used but with different angles $\theta/2 = 3\pi/4$ and $\theta'/2 = \pi/4$ and one output mode with coherent state amplitude $\beta = \sqrt{1/2}$. Next, one of the β modes is combined at a beam splitter with the β mode from the other state. The beam splitter has reflectivity $\cos^2\pi/4$, and the output modes are detected. The generation succeeds when only one photon is detected in total. If we perform an X correction on one of the modes the desired entanglement is produced with a probability of success of approximately 0.04.

An important feature of our noise model is the inclusion of two types of error: unlocated and located errors. A located error occurs when a gate fails. The experimenter has knowledge about when and where these errors occur. Unlocated errors are caused by photon loss as these errors are not directly observable. We have chosen to utilize the ''circuit-based telecorrector protocol'' described in [4] as this protocol has been designed to deal effectively with these types of errors. This protocol uses error-location information during ancilla-preparation and syndrome-decoding routines, thus achieving a high tolerance to located noise, while achieving a tolerance to unlocated noise similar to that of standard protocols [14,15]. In practice, other noise sources would be present, but the effect of these errors will be similar to those in our simplified noise model.

The probability of gate failure varies as a function of the input qubit state. For simplicity in the simulations, we apply the worst-case probability value, which corresponds to the input state $|+\rangle$. The maximum probability of failure (per qubit) for Z-basis measurements, and Clifford group operations [16] implemented by gate teleportation, is equal to

$$q = \frac{2}{1 + e^{2\alpha'^2}}. \tag{2}$$

In this equation $\alpha' = \sqrt{1-\eta}\alpha$ is an effective encoding amplitude which incorporates the effects of loss. Upon a gate failure the input qubit is erased. For simplicity we model this effect by completely depolarizing the qubit upon a located error occurring.

We model photon loss by assuming that each optical component, each detector, and each input coupling causes some fraction of the input intensity to be lost, and that this loss is equal for all modes. Because of the properties of a linear network with loss it is possible to assign one effective input coupling loss which incorporates all of this loss together. We also assume that the output of each gate includes the loss due to the detectors from the next gate or measurement. From this we can assign an effective input loss rate η which combines the detector, component, and input efficiencies together incorporating all these effects.

The effect of loss on a CSQC qubit is to induce a random Z operation and decrease the coherent state amplitude [17]. We assume that the decrease in amplitude is compensated by changing the amplitudes of the coherent states in the entanglement used for the teleported gates so that perfect interference is achieved with the input state and the output has the same coherent state amplitude as the input. However, after this correction the random Z operation sill persists. The probability of Z error on a diagonal CSQC state is

$$p = \frac{1}{2}\left(1 + \frac{\sinh(2\eta - 1)\alpha^2}{\sinh\alpha^2}\right), \tag{3}$$

where η is the overall fractional loss as defined above.

In the Z rotation and the controlled-Z gates, photon loss causes a Z error on the output state. These are due to the loss in the diagonal states from the generation of the entanglement. In the Hadamard gate, there are two diagonal states required, and a loss in one induces a X error on the output and a loss on the other induces a Z error on the output (these errors are uncorrelated).

In our analysis we consider two noise models which are summarized in Table I. We are considering here an error-correction protocol which consists of several levels of concatenation. The noise model in Table I applies only to the lowest level of concatenation. For all higher levels of concatenation, we assume a noise model identical to that considered in [4] for the ''circuit-based telecorrection protocol,'' since the arguments used to derive that noise model are applicable to our situation. Thus, our noise model and error-correction protocol are identical to that of [4] for concatenation levels 2 and higher, and so we do not perform new simulations for these levels.

For the first level of concatenation, we perform new numerical simulations, for the noise models in Table I. The simulator utilized the Monte Carlo method and was a modified version of the one used in [4] which incorporated the models considered here. All controlled-NOT gates were replaced by controlled-Z gates, and two Hadamard gates and simplifications of this circuit were performed. Separate simulations were performed for protocols based on the 7-qubit STEANE code and the 23-qubit GOLAY code [4,14]. The resulting threshold curves are shown in Fig. 3. An interesting feature is that increasing α beyond a certain point causes a reduced tolerance to photon loss.

Table II shows resource-usage estimates calculated during the numerical simulation for one round of error correction, for 5 levels of concatenation. An advantage of CSQC over LOQC is lower resource usage. Using Table II and the success probabilities in Fig. 2 we find that CSQC consumes approximately 10^4 diagonal resource states per error-correction round at the first level of con-

TABLE I. Error rates for the models used to calculate the threshold curve for CSQC. These error rates are determined by the calculated rate of a given error occurring in constructions shown in Figs. 1 and 2. The coefficients in the H gate and the C-Z gate arise from the larger α required for generating the entanglement and are worse case. The rows labeled $|+\rangle$ and X meas show the error rates for diagonal state preparation and X basis measurement, respectively. Models for qubit storage with photon loss (and without) are considered and shown in the row labeled ''Memory.''

	Loc. errors	Unloc. X error	Unloc. Z error
Memory	0	0	p or 0
H gate	q	$1.6p$	$1.6p$
C-Z gate	q	0	$2.5p$
$\|+\rangle$	0	0	p
X meas	0	0	0

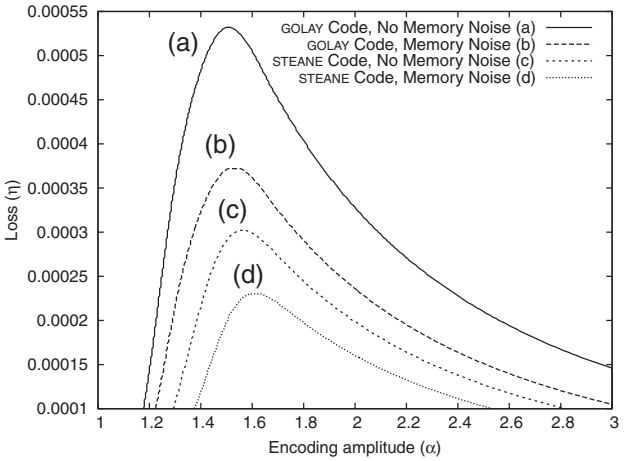

FIG. 3. Thresholds for CSQC using the 7-qubit STEANE and the 23-qubit GOLAY code for both memory noise models.

catenation. This approximation is calculated by multiplying the average number of diagonal resource states required to construct the resource for a particular operation by the number of times that operation is required and aggregating this result. This result is 4 orders of magnitude less than the number of Bell pair resource states consumed under equivalent conditions by the most efficient known LOQC scheme [4]. However, there is a trade-off. The photon loss threshold we find for CSQC is an order of magnitude smaller than that for LOQC. This means that if the loss budget is too large, then CSQC may not be scalable or may require so many levels of concatenation that the resource advantage is lost. We note that the physical resources in terms of specific optical states required to implement CSQC and LOQC are different. Nevertheless, we believe comparing resource state counts still gives a good estimate of the relative complexity of the two schemes. In future work, it would be valuable to include other sources of noise and improve upon some of the pessimistic assumptions made in deriving the noise model.

TABLE II. Effective error rates and resource usage for the 7-qubit STEANE code with memory noise enabled. The coherent state amplitude used for this table is $\alpha = 1.56$ and loss rate $\eta = 0.8 \times 10^{-4}$. This corresponds to gate error rates in our model of approximately (p, q). Resource usage is defined to be the total number of gates, preparations, measurements, and quantum memories used. Resources are used in the following fractions for all levels of concatenation: memory 0.284, Hadamard 0.098, controlled-Z 0.343, diagonal states 0.164, and X-basis measurements 0.111. Also shown is an estimate of the maximum length of computation possible assuming the entire computation succeeds with probability 1/2.

Level	Unloc. rate	Loc. rate	Max. comp. steps	Resource usage
1	4×10^{-4}	8×10^{-3}	82	1.0×10^{3}
2	1.7×10^{-4}	2×10^{-3}	3.3×10^{2}	8.7×10^{5}
3	2.8×10^{-5}	2.1×10^{-4}	3.0×10^{3}	4.5×10^{8}
4	7.4×10^{-7}	3.6×10^{-6}	1.6×10^{5}	2.1×10^{11}
5	5.3×10^{-10}	1.7×10^{-9}	3.1×10^{8}	9.6×10^{13}

We have shown how to construct a universal set of gates for CSQC for any coherent state amplitude. Provided the coherent state amplitudes are not too small ($\alpha > 1.2$) and photon loss is not too large ($\eta < 5 \times 10^{-4}$), it is possible to produce a scalable system. To our knowledge this is the first estimation of a fault-tolerance threshold for nonorthogonal qubits. As our gates work for all α, proof of principal experiments is possible using current technology.

We acknowledge the support of the Australian Research Council, Queensland State Government, and the United States Disruptive Technologies Office.

*lund@physics.uq.edu.au

[1] P. Kok *et al.*, Rev. Mod. Phys. **79**, 135 (2007).
[2] E. Knill *et al.*, Nature (London) **409**, 46 (2001).
[3] M. A. Nielsen, Phys. Rev. Lett. **93**, 040503 (2004); D. E. Browne and T. Rudolph, Phys. Rev. Lett. **95**, 010501 (2005); T. C. Ralph *et al.*, Phys. Rev. Lett. **95**, 100501 (2005).
[4] C. M. Dawson *et al.*, Phys. Rev. A **73**, 052306 (2006).
[5] T. C. Ralph *et al.*, Phys. Rev. A **68**, 042319 (2003).
[6] H. Jeong and T. C. Ralph, in *Quantum Information with Continuous Variables of Atoms and Light*, edited by N. J. Cerf, G. Leuchs, and E. S. Polzik (Imperial College Press, London, 2007).
[7] A. Ourjoumtsev *et al.*, Science **312**, 83 (2006); J. S. Neergaard-Nielsen *et al.*, Phys. Rev. Lett. **97**, 083604 (2006); K. Wakui *et al.*, arXiv:quant-ph/0609153; A. Ourjoumtsev *et al.*, Nature (London) **448**, 784 (2007).
[8] H. Jeong *et al.*, Phys. Rev. A **64**, 052308 (2001); H. Jeong and M. S. Kim, Phys. Rev. A **65**, 042305 (2002).
[9] C. H. Bennett *et al.*, Phys. Rev. Lett. **70**, 1895 (1993).
[10] I. D. Ivanovic, Phys. Lett. A **123**, 257 (1987).
[11] M. A. Nielsen and I. L. Chuang, Phys. Rev. Lett. **79**, 321 (1997).
[12] E. Knill, Nature (London) **434** 39 (2005).
[13] D. Aharonov and M. Ben-Or, in *STOC '97: Proceedings of the Twenty-Ninth Annual ACM Symposium on Theory of Computing* (ACM, New York, 1997), p. 176.
[14] A. M. Steane, Phys. Rev. A **54** 4741 (1996).
[15] B. W. Reichardt, arXiv:quant-ph/0406025.
[16] Non-Clifford group operations need not be implemented deterministically in the physical gates. They are needed only to generate an off-line resource state to implement their operation in a fault-tolerant manner (see M. A. Nielsen and I. L. Chuang, *Quantum Computation and Quantum Information* (Cambridge University Press, Cambridge, England, 2000), Chap. 10).
[17] S. Glancy *et al.*, Phys. Rev. A **70**, 022317 (2004).